



Numerical Simulation of Ocean Wave Using High-Order Spectral Modeling Techniques: Its Influence on Transport Sediment in Benoa Bay, Bali, Indonesia

Ulung Jantama Wisna^{1*}, Try Al Tanto¹, Widodo S. Pranowo², Semeidi Husrin², Gunardi Kusumah¹, Agus Maryono³

¹Research Institute of Coastal Resources and Vulnerability, Ministry of Marine Affairs and Fisheries

²Marine Research Center, Ministry of Marine Affairs and Fisheries, Indonesia

³Department of Civil and Environment Engineering, Faculty of Engineering, Gadjah Mada University, Indonesia

*Corresponding author: ulungjantama@gmail.com

Received 5 August 2018; Accepted 20 November 2019; Available online 26 November 2019

ABSTRACT

Benoa Bay is threatened by sedimentation issue within the bay by which it impairs the water mass circulation, influencing scour, mixing, and turbulence as well as sediment transport processes. This study aimed to determine the wave characteristic and its influence on the sediment transport within Benoa Bay. To conceive the wave characteristics, spectral wave modeling techniques were employed whereby the equation was discretized based on the condition of winds, tidal, and currents. Total sediment transport was calculated according to the wave model results. Total suspended sediment (TSS) model was simulated by considering bed load and suspended load intakes. Significant wave height (H_s) ranged 0-0.48 m and 0-0.44 m during high tidal condition and low tidal condition, respectively. Wave undulation propagates toward the West and Northwest within Bay. The wave period (T_s) ranged 2-6.5 second. Total sediment transport ranged 2828.16 - 86235.66 $m^3 \cdot year^{-1}$. TSS concentration ranged 1-100 $mg \cdot L^{-1}$ and 1-155 $mg \cdot L^{-1}$ during high tidal condition and low tidal condition, respectively. Those conditions indicate that the sedimentation has been extremely occurred within the bay. Some areas around Benoa peninsula, Benoa harbor, and Serangan Island are heavily polluted by suspended sediment. Bottom sediment is stirred by hydraulic jump off wave propagation by which its first wave crest induces scour and its train carries the stirred sediment entering the bay. If ongoing, this condition will exacerbate the existing ecosystem. Benoa Bay development has a big role evoking the level of TSS and turbidity. The more the sedimentation occurs, the more the ecological problem will take place.

Keywords: numerical simulation, ocean wave, spectral wave model, transport sediment, Benoa Bay

ABSTRAK

Teluk Benoa terancam masalah sedimentasi di dalam teluk yang mana hal tersebut menghalangi sirkulasi massa air, mempengaruhi gesekan dasar, pencampuran, dan turbulensi sedimen, serta proses transportasi sedimen. Penelitian ini bertujuan untuk mengetahui karakteristik gelombang laut dan pengaruhnya terhadap transportasi sedimen di dalam Teluk Benoa. Untuk mengetahui karakteristik gelombang laut, model spectral gelombang digunakan yang mana persamaannya didiskritisasi berdasarkan kondisi pasang surut, angin, dan arus laut. Transportasi sedimen total dihitung berdasarkan model gelombang yang telah disimulasikan. Total sedimen tersuspensi juga disimulasikan dengan mempertimbangkan masukan sedimen dasar dan sedimen melayang.

Tinggi gelombang signifikan (H_s) berkisar antara 0-0,48 m dan 0-0,44 meter pada kondisi pasang dan surut. Undulasi gelombang menjalar ke arah barat dan barat laut di dalam teluk. Periode gelombang signifikan (T_s) berkisar antara 2-6,5 detik. Total transpor sedimen berkisar antara 2828,16-86235,66 $m^3.tahun^{-1}$. Sedangkan untuk konsentrasi sedimen tersuspensi berkisar antara 1-100 dan 1-155 $mg.L^{-1}$ pada kondisi pasang dan surut. Kondisi tersebut mengindikasikan bahwa sedimentasi telah terjadi secara ekstrim di dalam teluk. Beberapa area disekitar tanjung Benoa, Pelabuhan Benoa, dan Pulau Serangan mengalami polusi suspesi sedimen. Sedimen dasar teraduk oleh lompatan hidrolik dari penjalaran gelombang dimana puncak gelombang terdepan menyebabkan gesekan dasar dan barisan penjalaran gelombang tersebut membawa sedimen yang teraduk untuk memasuki teluk. Jika berlangsung terus-menerus, kondisi ini dapat mengganggu ekosistem yang ada di Teluk Benoa. Pengembangan Teluk Benoa memiliki peran besar dalam peningkatan konsentrasi total suspensi sedimen dan kekeruhan. Semakin tinggi tingkat sedimentasi, maka masalah ekologi juga akan terjadi.

Kata Kunci: Simulasi numerik, gelombang laut, model gelombang spektral, transpor sedimen, Teluk Benoa

1. Introduction

Benoa Coastal Bay, located in the southern Bali Island, is severely strategic and potential to be developed in improving marine tourism in Bali Province. In fact, Benoa Bay has become the center of coastal development, tourism zone, and transportation for domestic and international interests. On the other hand, Benoa Bay has an important role in triggering imbalanced-environment because it becomes the last stream of rivers in the south Bali region. Moreover, there is a forest park (TAHURA) Ngurah Rai where some big rivers disembuged within Benoa Bay such as Badung River, Mati River, and Sama River (Rachman et al., 2016).

Benoa Bay is directly bordered by Lombok Strait and the Indian Ocean in the east and south, respectively whereby Lombok Strait is one of Indonesian throughflow (ITF) gates (Ningsih and Al Azhar, 2013). Some climatic variabilities such as El Nino Southern Oscillation (ENSO) and monsoons influence on hydrodynamic conditions in the surrounding Benoa Bay, particularly, in the generation of wind wave and its propagation from swell zone towards the coast. The changes in hydrodynamic conditions also are gradually caused by morphological alteration recently occurred in Benoa Bay (Wisha et al., 2017).

The development of Medane highway, connecting Kuta Regency, South Denpasar, Serangan Island and Benoa Harbor, triggers morphological alteration within Benoa Bay (Dharma and Candrayana,

2017). These changes directly impact on the hydrodynamic pattern formed. Generally, hydrodynamic Benoa Bay is predominated by tidal current (Hendrawan, 2005). Wave propagation also has an influence on evoking sediment transport because of the process of wave deformations (Sato and Liu, 2013). The strong wave, passing swell zone area, moves toward the bay mouth through Serangan Island and Benoa Peninsula. The wave propagation, triggering scour event and turbulence beneath the first wave crest, moves toward the bay, resulting in higher sedimentation rate in the bay mouth and within the bay. That is why it is often dredged by the Benoa Port management (Dharma and Candrayana, 2017).

It is necessary to establish a comprehensive understanding, dealing with the phenomenon occurred in the coastal zones, in order to avoid the negative impacts. One of the common solutions is the modeling approach. The approach does not need much space. Therefore, it is cheap and efficient. Besides, it can easily perform a variety of either assumptions or scenarios required (Crespo, 2008). The modeling approach also gives an advantage in finding a solution to solve complicated problems effectively and efficiently in the hydrodynamic processes in the ocean (Cummins et al., 2012). In this case, it is applied in the wave simulation of Benoa Bay, Bali.

Several previous related studies have been published. Discroll et al. (1998)

discussed the reclamation of Turtle Island. Hendrawan (2005), defined the water circulations within Benoa Bay. Hendrawan and Ardana (2009) simulated the phosphate transport within Benoa Bay using numerical simulation. Ningsih and Al Azhar (2013) modeled hydrodynamic within Benoa Bay. Hendrawan and Asai (2014) simulated the tidal current pattern and seawater exchange in the Benoa Bay. While, Hendrawan et al. (2016) defined the characteristics of total suspended sediment and turbidity within the bay. The other research by Rachman et al. (2016) and Dharma and Candrayana (2017) modeled sediment transport within Benoa Bay. The last study was conducted by Al Tanto et al. (2017) defined the character of sea current and tidal current modeling. Wisha et al. (2018) simulated the reclamation impact on tidal current pattern changes. Therefore, conducting a study revealing the wave's characteristics to describe its impacts on sedimentation processes induced by the development of Benoa Bay is essential. Thus, this study aimed to determine the characteristic of ocean waves and its influence on the sediment transport within Benoa Bay.

2. Materials and Methods

2.1 Spectral wave equations

In the Spectral Wave (SW) model, the wind wave is represented by the density spectrum of wave propagation $N(\sigma, \theta)$. Independent parameter phase was chosen as a relative angular frequency (Intrinsic), $\sigma = 2\pi f$ and the direction of wave propagation, θ . The relation between relative angular frequency and absolute angular frequency, ω , is given by the linear dispersion relationship as follow:

$$\sigma = \sqrt{gk \tanh(kd)} = \omega - k.U$$

Where g is the gravity acceleration, d is the water depth, U is the vector of current velocity, k is the wave vector value with the velocity of k and the direction of θ . Density action, $N(\sigma, \theta)$ is related to the density of energy $E(\sigma, \theta)$ as follow:

$$N = \frac{E}{\sigma}$$

The governing equation in the SW model is equalized from wave equation formulated between Cartesian and Spherical coordinates. While, in the horizontal Cartesian coordinate, the conversion of wave equation is given as follow:

$$\frac{\partial N}{\partial t} + \nabla \cdot (vN) = \frac{S}{\sigma}$$

Where $N(x, \sigma, \theta, t)$ is a density, t represents the time, $x = (x, y)$ is a Cartesian coordinate, $v = (C_x, C_y, C_\sigma, C_\theta)$ is the wave group propagation velocity in the 4-dimensions of phase of x, σ, θ . And S is the source of energy equilibrium equation. ∇ is the differential operator 4 dimensions in the x, σ, θ directions. The propagation speed of wave is given by the kinematic linear relationship as follow:

$$\begin{aligned} (c_x, c_y) &= \frac{dx}{dt} = \tau g + U \\ &= \frac{1}{2} \left(1 + \frac{2kd}{\sinh(2kd)} \frac{\sigma}{k} \right) + U \\ c_\sigma &= \frac{d\sigma}{dt} = \frac{\partial \sigma}{\partial d} \left[\frac{\partial d}{\partial t} + U \nabla_x d \right] - c_g \cdot k \cdot \frac{\partial U}{\partial s} \end{aligned}$$

$$c_\theta = \frac{d\theta}{dt} = -\frac{1}{k} \left[\frac{\partial \sigma}{\partial d} \frac{\partial d}{\partial m} + k \cdot \frac{\partial U}{\partial m} \right]$$

Where, s is the coordinate distance in the wave direction θ , m is the perpendicular coordinate to S . $\nabla_x d$ is the two-dimensions differential operator in the x -direction. Wave conservation integrated from all model area ($\Delta\sigma t$) and the interval of propagation direction ($\Delta\theta m$) are discretized as follow:

$$\begin{aligned} \frac{\partial}{\partial t} \int_{\nabla\theta m} \int_{\Delta\sigma t} \int_{A_i} N d\Omega d\sigma d\theta \\ - \int_{\Delta\theta m} \int_{\Delta\sigma t} \int_{A_i} \frac{S}{\sigma} d\Omega d\sigma d\theta \\ = \int_{\Delta\theta m} \int_{\Delta\sigma t} \int_{A_i} \nabla \cdot (vN) d\Omega d\sigma d\theta \end{aligned}$$

Where, Ω is the integration of wave variable resulted by A_i , using a divergent

theory and showing the convective flux $F = vN$, the discretization is developed as follow:

$$\frac{\partial Ni,l,m}{\partial t} = -\frac{1}{Ai} \left[\sum_{p=1}^{NE} (Fm)p,l,m \nabla lp \right] - \frac{1}{\Delta\sigma l} \left[(F\sigma)i,l,m + \frac{1}{2} - (F\sigma)i,l - 1/2,m \right] - \frac{1}{\Delta\theta m} \left[(F\theta)i,l,m + \frac{1}{2} - (F\theta)i,l,m - 1/2 \right]$$

Where NE is the total value of refraction on cell, $(Fn)p,l,m = (Fxn + Fyny)y.l,m$ is the normal flux beyond the refraction p within geographic coordinate and the length of Δlp . $(F\sigma)i,l + \frac{1}{2},m$ and $(F\theta)i,l,m + \frac{1}{2}$ are the flux passing the front part of direction frequency, respectively.

2.2 Spectral wave model materials and preparation

Wind data were obtained from BMKG (Meteorological, Climatological, and Geophysical Agency of Indonesia). These wind data were then sorted and used for simulating hydrodynamic model in the form of time series data (dfs0). Theoretically, winds are the main factor triggering the surface dynamic of water (Wisha et al., 2015). Wind transfers its energy through sea surface, forming the wind wave after passing the wave's breaking zone. Its energy propagates and forms longshore currents. Wind direction dominantly moves towards Northeast, Southeast, and Southwest, with the speed averagely ranged from 0-15 m/s (Figure 1). The statistic descriptive of wind data are shown in Table 1.

The tidal prediction was employed to generate the time series of water level data. Data were predicted from field measurement to extract tidal constituent and predict surface elevation (Hendrawan and Koji, 2014). From the tidal model, the extraction of tidal harmonic constituent and the prediction of tidal elevation in the given location and time are possible. The tidal forecasting was also applied before the study to establish tidal patterns. It was then

compared with field data to analyze the tidal phase (Jun-Zheng and Pu-bing, 2009).

Table 1. Statistic descriptive of wind data implemented in the model simulation

Parameter	Value
Max wind speed (m.s ⁻¹)	7.20
Min wind speed (m.s ⁻¹)	0
wind speed average (m.s ⁻¹)	3.151
Wind direction average (Degree)	93.77
Total data (n)	172
ST dev.	±1.4

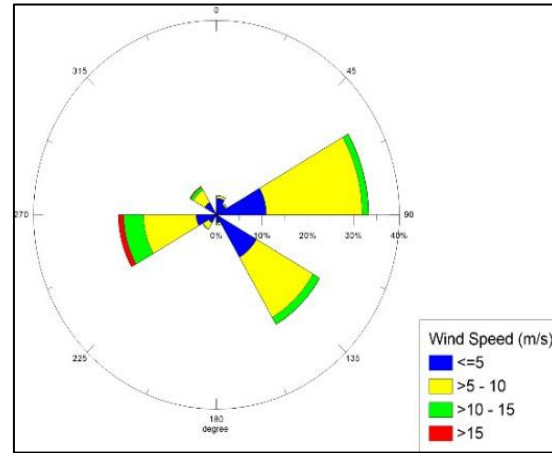


Figure 1. Wind rose diagram of annual wind data

A boundary condition in the model was established, namely the east regional boundary. This eastern boundary condition was represented by field tidal data which were then forecasted along the boundary. Processed data in this study were obtained from direct measurements in the field and secondary data.

Oceanographic data were implemented to validate the SW model by comparing the field data and model results. The SW simulation applied the 2-dimensional horizontal numerical approach. From the SW model results, one of the observation points was sampled to validate the model result, adjusted by location point of field measurement (Lazure et al., 2009). The set-up implemented in the SW model is shown in Table 2.

Table 2. Spectral wave model set-up

Parameters	Implemented in the simulation
Time of simulation	No. of time steps = 86400 Time step interval = 10 sec Simulation start date = 1/05/2016 00.00 AM Simulation end date = 11/05/2016 00.00 AM
Basic equations	Spectral formulation = Fully spectral formulation Time formulation = In stationary formulation
Spectral discretization	Frequency discretization - equisidant = 1. Number of frequencies 25 2. Minimum frequency 0.055 Hz 3. Frequency interval 0.02 Hz Directional discretization = 360 degree rose 16 directions Separation of wind and swell-constant threshold frequency 0.125 Hz
Solution technique	Max number of levels in transport calculation 32 Number of steps in source calculation 1 Minimum time step 0.01 sec Maximum time step 10 sec
Water level condition	Varying in time, constant in domain= tide forecasting with coordinate: Longitude: 115.260 East, Latitude: 8.755 South Longitude: 115.248 East, Latitude: 8.800 South
Wind forcing	Varying in time, constant in domain = wind data time series (speed and direction)
Energy transfer	Include quadruplet-wave interaction Include triad-wave interaction-transfer coefficient 0.25
Bottom friction	Sand grain size d50-constant value 0.00025 m
Boundary condition	Wave parameters: Significant wave height, Hm0 0.4 m. Peak wave period, Tp 8 sec. Mean wave direction, MWD 45 degree Directional spreading index, n 5

2.3 Sediment transport calculation

Sediment transport along the coast was calculated by employing empirical equation developed based on model result data and the prototype for sandy beach. This equation is a correlation between sediment transport and wave's energy flux component in the form of flux equation (Triatmodjo, 2012) as follow:

$$P_1 = \frac{\rho g}{8} H_b^2 C_b \sin \alpha_b \cos \alpha_b$$

where:

P_1 = wave energy flux component along the coast at the time of breaking ($kg.m/d$)

ρ = specific gravity of sea water (kg/m^3)

g = acceleration of gravity = 9.81 (m/s^2)

H_b = breaking wave height (m)

C_b = breaking wave celerity (m/s) = $\sqrt{gd_b}$

α_b = breaking wave angle

To calculate total sediment transport annually, a formula developed by Triatmodjo (2012) was employed. The distribution of sediment is applied in the vastly surf zone, where sediment transport is slightly hard to determine. That formula is discretized only for a homogenous sandy beach, the diameter average varies ranged 0.175-1 mm. The formula to calculate total sediment transport is developed by Triatmodjo (2012) as follow:

$$Q_s = \frac{K}{(\rho_s - \rho)g(1 - n)} P_1$$

where:

Q_s = sediment budget along the coast (m^3/s)

$K = 0.39$, in which the formula above used significant wave height value

ρ_s = Specific gravity of sand (kg/m^3)

n = Porosity ($n \approx 0.4$)

Total suspended sediment model was simulated to prove the sediment transport calculation above which based on the consideration of bed and suspended loads. The model applied will calculate the sediment load separately. It is then summed to obtain the total load based on the sediment load concentration as follow:

$$\begin{aligned} \frac{\partial C_i}{\partial t} + \frac{\partial u C_i}{\partial x} + \frac{\partial v C_i}{\partial y} + \frac{\partial (w - w_i) C_i}{\partial z} \\ = \frac{\partial (A_u \frac{\partial C_i}{\partial x})}{\partial x} + \frac{\partial (A_u \frac{\partial C_i}{\partial y})}{\partial y} \\ + \frac{\partial (K_h \frac{\partial C_i}{\partial z})}{\partial z} \end{aligned}$$

where:

C_i = Concentration value of suspended sediment

A_u = Horizontal Eddy viscosity

K_h = Vertical Eddy viscosity

$w - w_i$ = Settling velocity adjusted with sediment type applied in the model

In the surface layer, the value of flux boundary condition used $K_h \frac{\partial C_i}{\partial x} = 0, z = \zeta$, for bed layer, the value of sediment flux has a different deposition and erosion. For deposited sediment, it used the value of $K_h \frac{\partial C_i}{\partial x} = E_i - D_i, z = \zeta$, and for the eroded sediment, it used the formula of $E_i = \Delta t Q_i (1 - P_b) F_{bi} (\frac{\tau_b}{\tau_{ci}} - 1)$, which Q_i is erosion flux, P_b is porosity in the bottom waters, F_{bi} is fraction of bottom sediment, τ_b is the pressure of bottom shear stress, and τ_{ci} is the critical shear stress of sediment.

2.4 Field measurement and observation stations

Waves, currents, and tides were recorded using Acoustic Doppler Current Profiler (ADCP) deployed in the 3 observation stations (Figure 2). The measurement was conducted by PT. Tirta Wahana Bali International (TWBI), while the ADCP Aquadopp - NORTEK is installed for 21-days measurement (Table 3). TSS field data was obtained from previous research, conducted by both Rachman et al. (2016) and TWBI at the same time of ADCP deployment. These data were used for TSS model validation. The tidal data were analyzed by employing admiralty method, used as an input in the model simulation. ADCP data measurement results were applied as the basis data of SW model validation. The validation was done by employing Root Mean Square Error (RMSE) formula as follow:

$$RMSE = \sqrt{\frac{1}{N} \sum_{i=1}^N (x_i - y_i)^2}$$

where:

N = The number of total data

x_i = Model result

y_i = Field measurement data

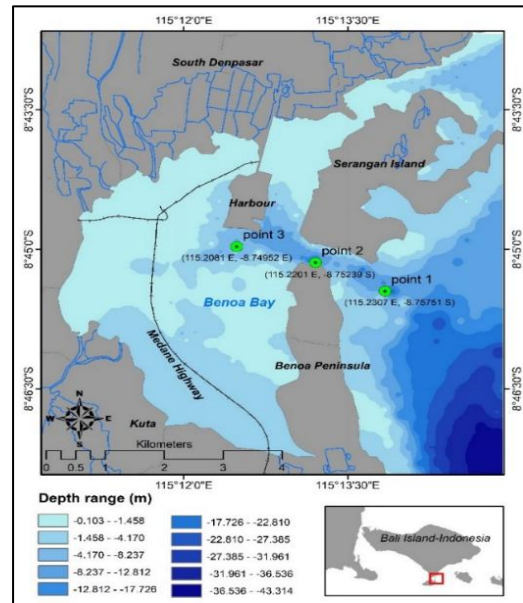


Figure 2. Research location map

Table 3. The location and the measurement period of ADCP

Location	The depth of ADCP deployment	The date of measurement	Moon condition
ADCP 1	13.3 m	June, 20-30 th 2015	Neap
ADCP 2	13.3 m	June, 25 th – July, 11 th 2015	Neap and Spring
ADCP 3	11.6 m	July, 2 nd -3 rd 2015	Spring

3. Result and Discussion

3.1 Model validation

The model result must be validated before it applied to figure out the study area. The validation was done by comparing the field data (from ADCP) with the model result (Gao et al., 2009). The value of Root Mean Square Error (RMSE) obtained of 9.74 % for surface elevation data (Figure 3). Figure 3 shows that the phase comparison at the

neap tidal condition is slightly different due to the wave influences. According to Garrett and Kunze (2007) the surface elevation changes are followed by the wave generation, usually contribute to the characteristics of elevation formed. The validation is also applied employing the linear regression method (Figure 4), which it shows the R-square value obtained of 0.78. That value defines that the two-data compared are closely similar (78 % similarities in phase and elevation).

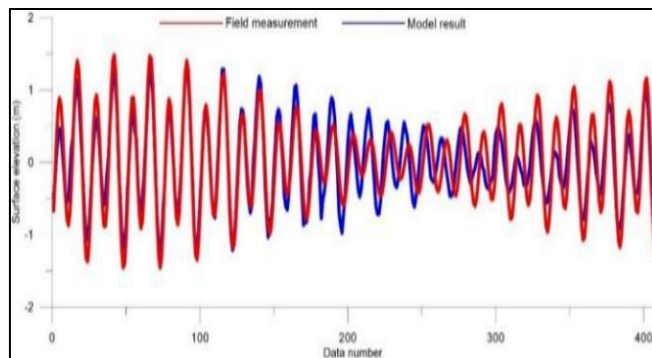


Figure 3. Model verification using surface elevation data

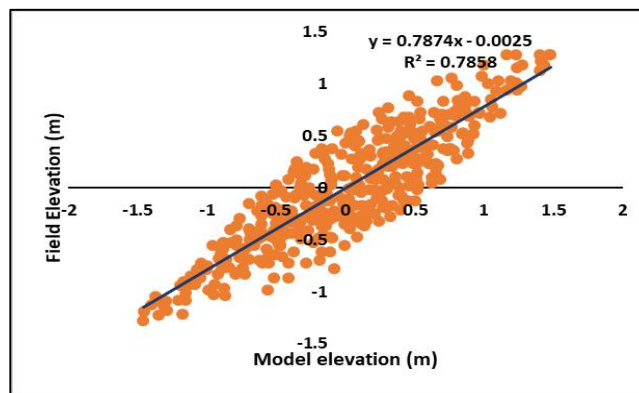


Figure 4. Linear regression assessment of surface elevation data

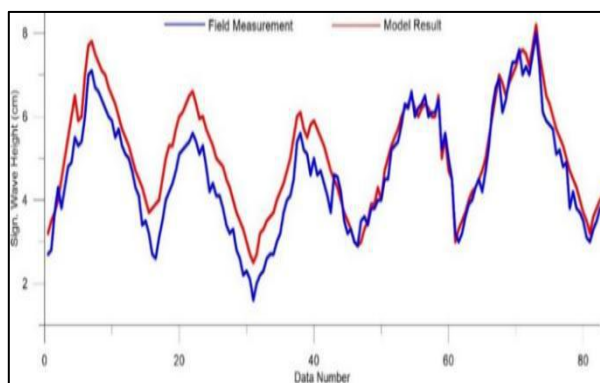


Figure 5. SW model verification using significant wave height data

The SW model was validated by comparing the wave data obtained from TWBI with the model result. The RMSE obtained of 12.49 % for significant wave height data comparison (Figure 5). The field data (blue line) looks more fluctuate, it is because of the influence of surface wind during the measurement time. Wind wave generation and propagation, subsequent depth-limited breaking, and the associated transfer of the wind wave momentum through wave radiation stress gradient forcing, influence on surge elevation, currents circulation, and modify the peak surge (Bunya et al., 2010). According to (Warner et al., 2010) water levels, currents, and wind waves will affect wave's generation and transformation.

3.2 Spectral Wave (SW) simulation

Benoa Harbor and Medane Toll highway, connecting 2 vital regions (Kuta and South Denpasar), have been built. In general, the development implemented affects to the formation of hydrodynamic pattern. At the condition of maximum water level, significant wave height ranged 0-0.48 meters (Figure 6) and 0-0.44 meters when the water level

decreased (Figure 7). The domination of waves direction is relatively stable in every water level condition, propagating westward and northwestward within the bay.

Hs value is lower reached 0.08 meters during the high and low tidal condition around the bay mouth. The wave group propagation energy forms longshore current stream (Jose et al., 2007). At the low tidal condition, several areas within the bay (red circle) (Figure 7) become dry where there is no water covered over the bay.

At station 1, the Hs value ranged 0-0.3 meters (Figure 8), at station 2, the Hs value ranged 0-0.08 meters (Figure 9) and at station 3, the Hs value ranged 0-0.02 meters (Figure 10). It proves that the value of Hs will decrease in line with the depth reduction. The existence of bed resistance causes wave deformations such as shoaling effect and refraction in the bay mouth (Ondara and Wisha, 2016). Besides, waves will be diffracted around Medane highway foundation, will evoke sedimentations behind.

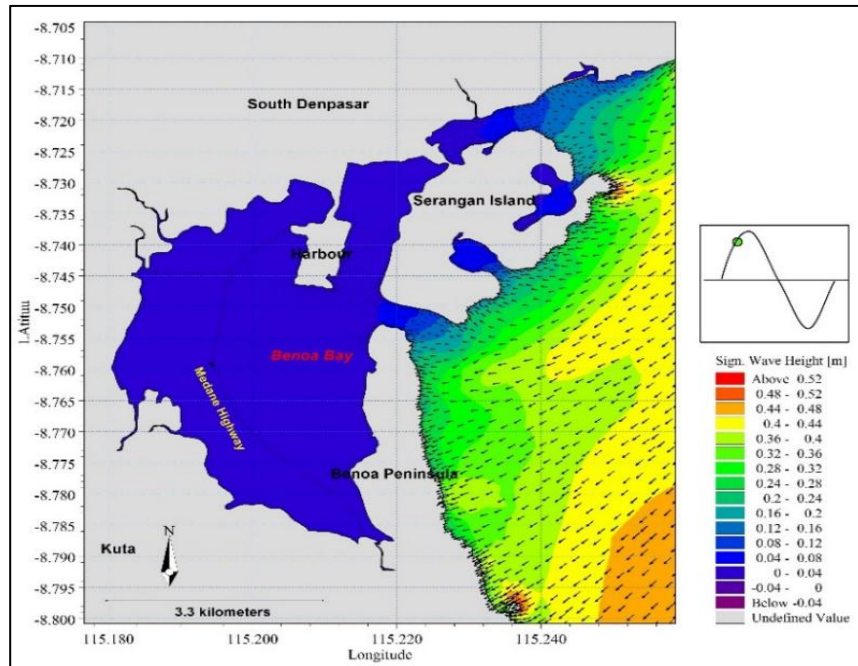


Figure 6. Shallow water wave simulation at the maximum water level condition

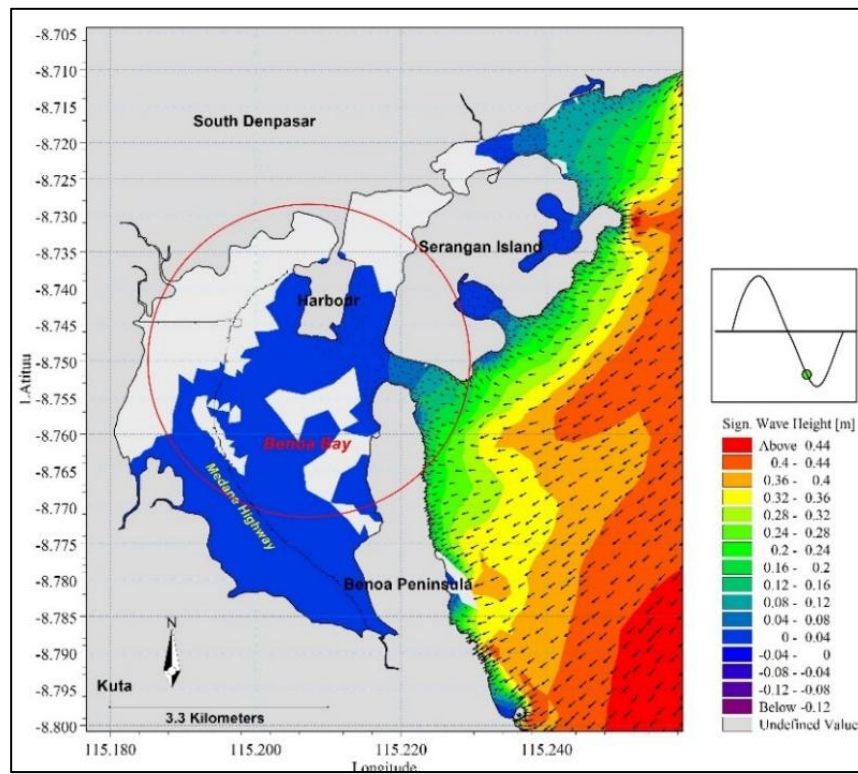


Figure 7. Shallow water wave simulation at the minimum water level condition

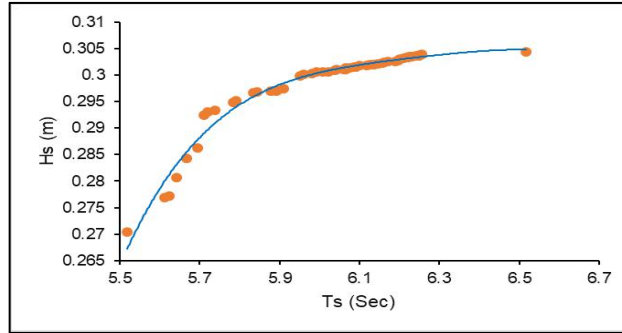


Figure 8. Wave period and significant wave height at station 1

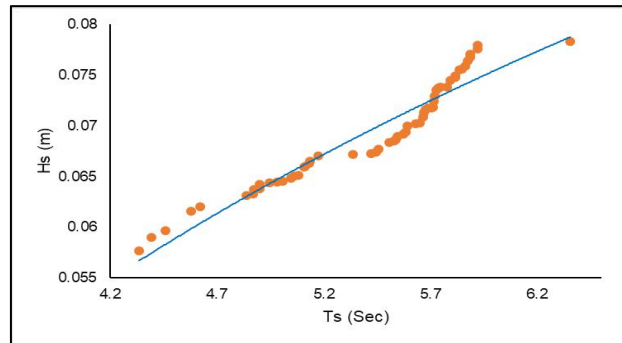


Figure 9. Wave period and significant wave height at station 2

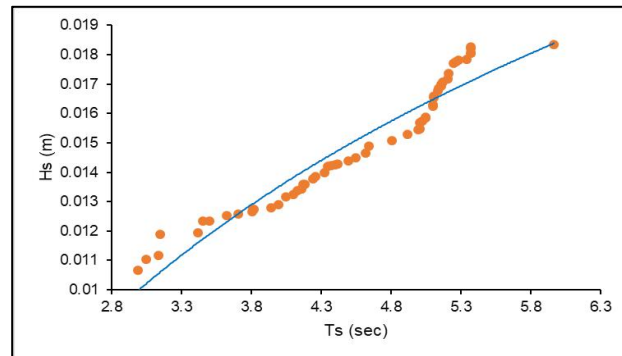


Figure 10. Wave period and Significant wave height at station 3

At each observation station, the result shows that the H_s value is inversely proportional to the significant wave period (T_s). The wave period is also affected by the wavelength (λ) (Meylan et al., 2014). The increase of H_s value results a greater wavelength and the wave period becomes longer, nevertheless, it also depends on its energy and velocity (Ondara and Wisha, 2016).

At station 1, H_s value is greater than station 2 and 3. The period span is faster averagely 1.0 second (Figure 8). T_s value ranged from 5.5-6.5 seconds. At station 2, T_s

value is lower of 1.9 seconds (Figure 9), while the period is longer than station 1 due to the depth changes and deceleration of wave group velocity. At station 3, H_s value is the lowest, while the T_s value reached 2.0 seconds, it is longer compared to the other point, T_s value ranged 4.4-6.4 seconds (Figure 10). Station 3 located within the bay is tremendously shallow. The wave group velocity gradually reduces because of shoaling and waves deformation occurred in the bay mouth (Triatmodjo, 2012; Ondara and Wisha, 2016).

The wavelength of wave group dispersed in the x and y directions is also different. At station 1, the celerity is greater which a negative dispersion value is identified (Figure 11A). At station 2, the celerity decreases and positive dispersion takes place (Figure 11B). While, at station 3, the celerity decreases drastically (almost reaching zero dispersion) which almost does not exist as well as in the negative condition (Figure 11C). The dispersions occurred are more irregular even though it has a different velocity, which it is sufficiently stable at station 2.

3.3 Sediment transport calculation based on the model results

Total sediment transport was calculated based on the SW model simulated before. Firstly, the wave energy flux

component after passing the breaking zone were determined at each station, the gained values are 67.06; 9.43; 2.20 kg.m.s⁻¹, respectively (Table 4). The energy was bigger at station situated without the bay and declined gradually in the bay mouth and within the bay, these conditions may result in different dramatic sediment transport volume. Outside area of Bena Bay (station 1), total sediment transport reached 86235.66 m³.year⁻¹. In the bay mouth (station 2) reached 12126.96 m³.year⁻¹, while, within the bay reached 2828.16 m³.year⁻¹ (station 3). It is obvious why the sediment transport is more erratically without the bay due to the higher energy flux, wind pressure, and water circulation occurred in Lombok Strait (Ningsih and Al-Azhar, 2013).

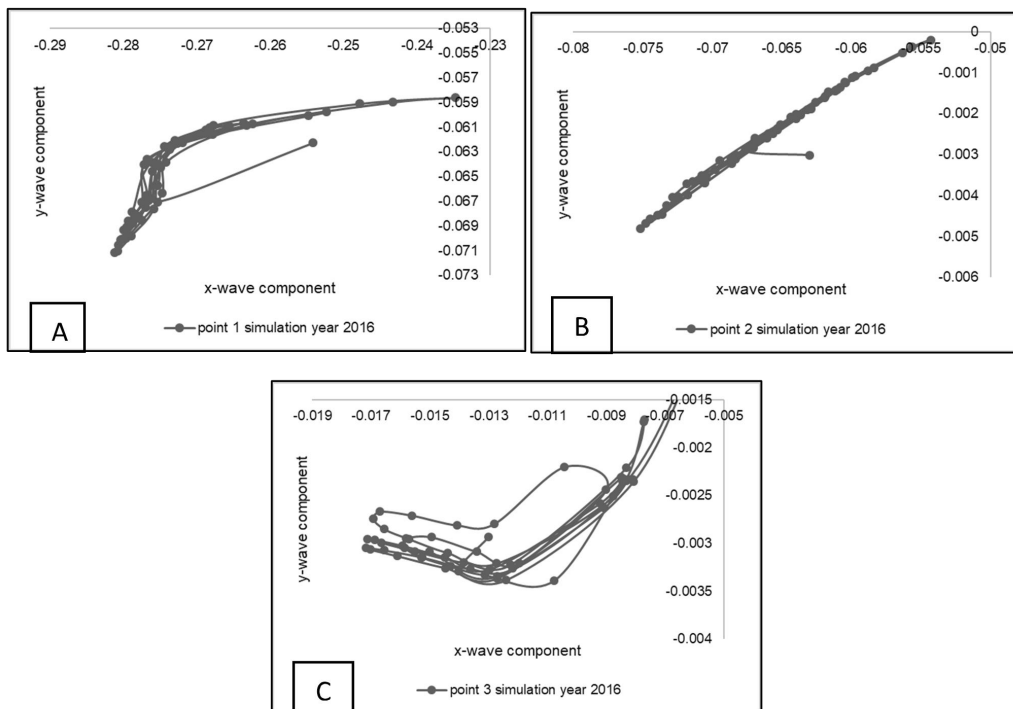


Figure 11. Scatter plot of wave component for (A) station 1, (B) station 2 and (C) station 3

Scour event occurred without the bay is caused by the hydraulic jump off wave propagation, inducing bed sediment turbulence beneath the first wave crest (Qi and Gao, 2014; Docherty and Chanson, 2010). The scoured sediment is transported toward the bay, resulting in deposited sediment in the shallower area. According to Braden (2015) Eddy diffusivity

(dispersing tendency) in the turbulent flow accounts for sediment suspension, mixing, and transportation. The turbulence intensity is presented by the velocity of the random jumps, and the mixing length by the length of the jumps. Since turbulence is a comparative phenomenon, some regions within the bay will have lesser turbulence than others, and in the

regions of more turbulence, there will be no sedimentation (without Benoa Bay).

The minimal sediment transport within the bay indicates that the high sediment deposition is triggered by the low water dynamics. It explains that the area is not covered by water during the low tidal condition. It is the reason why in this area, it planned to be reclaimed several years to go. On the other hand, the water mass transport hardly takes place passing the bay mouth. Generally, the tremendous weak water mass dynamic within a bay will trigger the increase of sedimentation (Kartadikaria et al., 2011).

Wave propagation and deformation are influenced by the bathymetry profile (Ricchiuto and Filippini, 2014). The average of water depth ranged from 0-5 meters (shallow water) within the bay. Bottom friction has a significant role in controlling wave growth in the coastal area. According to Zijlema et al. (2012), bottom friction controls the magnitude of velocity component. It varies over the seabed according to bathymetry profile dissipating energy in a thin and turbulent boundary layer of surface bottom.

When the waters become shallow, the water mass dynamics tend to be weak because the bottom friction stress takes place. The weakened flow dynamics within the bay causes the distribution of sediment and suspended matter ease, and eventually, it settles and accumulates in the bottom (Braden, 2015). It will trigger sedimentation phenomena due to the lesser turbulence and mixing within the bay.

Total suspended sediment (TSS) model was validated by comparing the three TSS data sources, *i.e.* TSS resulted from simulation, TWBI measurement result and previous research published by Rahman et al. (2016) (Figure 12).

The comparison shows that the same pattern of the lowest TSS concentrations is identified at station 1. While, the highest TSS concentration is identified at station 3. It indicates that the high turbulence is occurred without the bay and then transported toward within the bay. If ongoing, these conditions will jeopardize biota existence, and induce water quality degradation as well as biogeochemical cycles disruption in the Benoa Bay.

Table 4. Total sediment transport calculation result

Observation points	P_1 ($kg.m.s^{-1}$)	Q_s		
		$m^3.day^{-1}$	$m^3.month^{-1}$	$m^3.year^{-1}$
Point 1	67.06	273×10^{-5}	236.26	86235.66
Point 2	9.43	38×10^{-5}	33.22	12126.90
Point 3	2.20	8.968×10^{-5}	7.75	2828.16

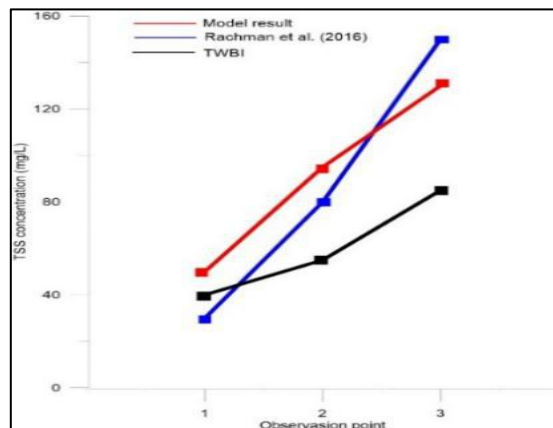


Figure 12. TSS model result compared with previous research and field measurement

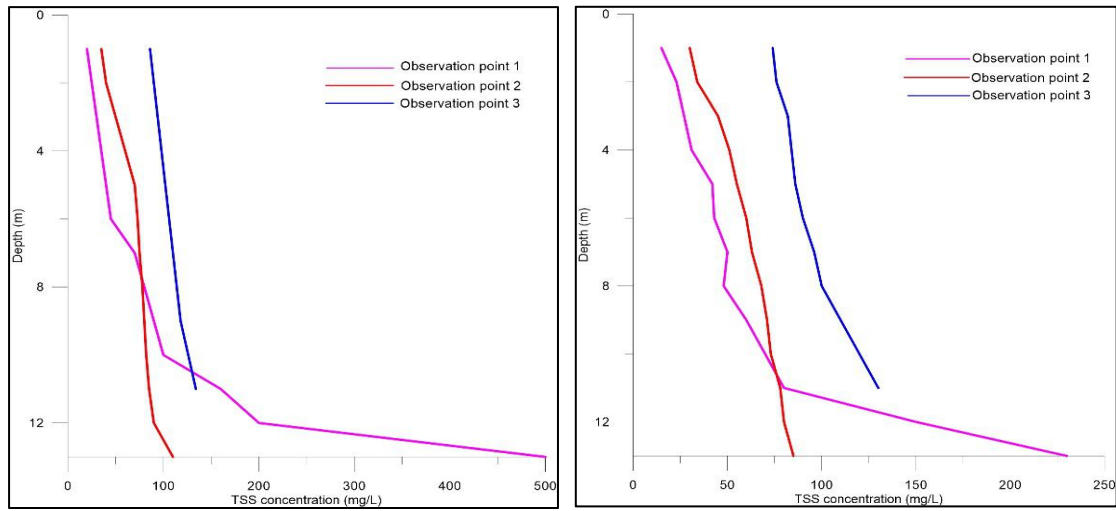


Figure 13. TSS vertical profile during the high tidal condition (left) and the low tidal condition (right)

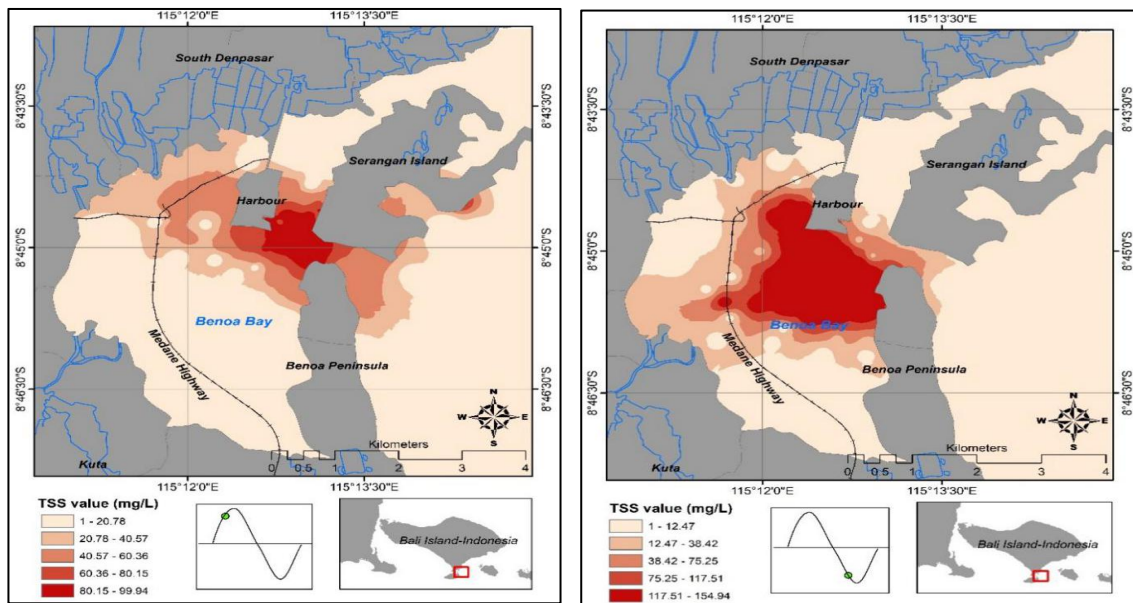


Figure 14. TSS distribution at the high tidal condition (left) and the low tidal condition (right)

TSS vertical profile within Benoa Bay varies in every elevation change, it was higher during the low tidal condition ranged 20-500 mg/L and lower during the high tidal condition ranged 15-230 mg/L (Figure 13). At station 1, the highest TSS concentration is identified in the surface bottom, while, it significantly declines in the surface water. On the other hand, vertical TSS trend is not dramatically changed, although the stable

high concentration is still identified at station 3. During the high tidal condition, maximum TSS concentration is also founded at station 1 near the surface bottom reached 230 mg/L. This condition indicates that the intense turbulence and resuspension events frequently occurred during the low tidal condition (Chao et al., 2013). Moreover, the sediment resuspension in the regional scale

is controlled by the wave propagation (Warner et al., 2010).

Figure 14 shows the distribution of TSS around Benoa Bay. TSS concentration is centered near Benoa Harbor ranged 80-100 mg/L and 117-150 mg/L during the high tidal condition and the low tidal condition, respectively. At the low tidal condition, elevation pressure becomes higher and triggers turbulence within the bay. It is obvious why the concentration of suspended sediment is higher in the shallower waters. The breaking waves, propagating the bay in the form of longshore currents, have a big role in controlling sediment transport in Benoa Bay (Wisha et al., 2017) which it might evoke erosion and sedimentation in several areas within the bay.

The area between the Benoa peninsula, Benoa harbor and Serangan island is heavily polluted by suspended sediment (Figure 14). The higher concentration of TSS is centered in the bay mouth due to the higher water mass movement in the convergence (V-shaped) area, inducing a tremendous transport and sedimentary turbulence which is then transported and settled within the bay, resulting in higher sedimentation rates and decreasing the water depth (shallower). The higher TSS pollution in the coastal area will induce environmental issues and disrupt the biogeochemical processes. According to Chen et al. (2009), TSS is a major factor deteriorating phytoplankton photosynthesis intensity and indirectly predisposes the other biota in the food chain. The abundance of phytoplankton is inversely proportional with TSS, turbidity, and suspended materials (Wisha et al., 2016).

4. Conclusion

Waves propagation predominantly moves toward Benoa Bay with a constant value of significant wave height and wave period, triggering transport mechanism within the bay. The higher bed load sediment in the swell region is stirred due to the hydraulic jump off wave propagation. The stirred sediment will be transported and settled within the bay, enhancing sedimentation in the shallower area. The area within the bay was planned to be reclaimed in the intertidal area. It is because

these areas were not covered by water during low tidal condition, indicating extreme sedimentation within the bay, mainly occurred around the bay mouth (surrounded by Benoa Harbor, Peninsula, and Serangan Island). If ongoing, this condition will exacerbate the ecosystem. Furthermore, the development in Benoa Bay has a big role in evoking the higher level of TSS and turbidity whereby Benoa Bay condition will be more deteriorate.

This study can be useful for local government by which consideration of reclamation planning and impacts, and also ecosystem mitigation due to the development of Benoa Bay is essential. Dredging is also necessary to control the sedimentation within the bay because this condition will disrupt the vessel transportation in and out Benoa Bay.

Acknowledgement

Acknowledgments and gratitude are given to PT. Tirta Wahana Bali International (TWBI) for sharing the field measurement data (tides, waves, and TSS) and Research Institute for Coastal Resources and Vulnerability (RICSV) for research funding 2016 in Benoa Bay, for those who support the completion of this article and for every institute which support in completing the main data.

References

- Al Tanto, T., U. J. Wisha, G. Kusumah, W. S. Pranowo, S. Husrin, I. Ilham, A. Putra. 2017. Sea Current Characteristics of Benoa Bay - Bali. *Jurnal Ilmiah Geomatika* 23(1), 37-48.
- Braden, G. E. 2015. Turbulence, diffusion and sedimentation in stream channel expansions and contractions. In *Proceedings of the Oklahoma Academy of Science* 31: 73-77.
- Bunya, S., J. C. Dietrich, J. J. Westerink, B. A. Ebersole, J. M. Smith, J. H. Atkinson, R. Jensen, D.T. Resio, R.A. Luettich, C. Dawson, V.J. Cardone, A.T. Cox, M.D. Powell, H.J. Westerink, H.J. Roberts. 2010. A high-resolution coupled riverine flow, tide, wind, wind wave, and storm

- surge model for southern Louisiana and Mississippi. Part I: Model development and validation. *Monthly weather review* 138 (2): 345-377.
- Chao, W., Chao, S., Wang, P. F., Jin, Q., Jun, H., LIU, J. J. 2013. Modeling of sediment and heavy metal transport in Taihu Lake, China. *Journal of Hydrodynamics, Ser. B* 25 (3): 379-387.
- Chen, Z., C. Hu, F. E. Muller-Karger, and M. E. Luther. 2010. Short-term variability of suspended sediment and phytoplankton in Tampa Bay, Florida: observations from a coastal oceanographic tower and ocean color satellites. *Estuarine, Coastal and Shelf Science* 89 (1): 62-72.
- Crespo, A. J. C. 2008. Application of the smoothed particle hydrodynamics model SPHysics to free surface hydrodynamics. (PhD Thesis). Universidade de Vigo. Departement of Applied Physic. Manchester. United Kingdom.
- Cummins, S. J., T. B. Silvester., P. W. Cleary. 2012. Three-dimensional wave impact on a rigid structure using smoothed particle hydrodynamics. *International Journal for Numerical Methods in Fluids* 68 (12), 1471-1496.
- Dharma, I. G. B. S., W. Candrayana. 2017. Hydrodynamics and Sediment Transport of Benoa Bay, Semi-Enclosed Bay in Bali, Indonesia. In *Applied Mechanics and Materials* 862: 3-8. Trans Tech Publications.
- DHI. 2013. MIKE 21 & MIKE 3 Flow Model FM Hydrodynamic Module - Short Description. DHI Headquarters Agem Alle 5. DK-2970 Horsholm. Denmark.
- Docherty, N. J., Chanson, H. 2010. Characterization of Unsteady Turbulence in Breaking Tidal Bores Including the Effects of Bed Roughness. *Hydraulic Model Reports*. School of Civil Engineering, The University of Queensland, Report CH76/10. 100 pp.
- Gao, J. X. Lan, Y. Fan, J. Chang, G. Wang, C. Lu., C. Xu. 2009. CFD modeling and validation of the turbulent fluidized bed of FCC particles. *AIChE Journal*, 55(7), 1680-1694. Doi: 10.1002/aic.11824.
- Garrett, C., E. Kunze. 2007. Internal tide generation in the deep ocean. *Annual Review of Fluid Mechanics* 39: 57-87.
- Hendrawan, I. G. 2005. Barotropic Model to Calculate Water Circulation in Benoa Bay, Bali (Doctoral dissertation. (Thesis). Master Program of Environmental Study, Udayana University, Denpasar, Bali.
- Hendrawan, I. G., I. K. Ardana. 2009. Numerical calculation of phosphate transport in Benoa Bay, Bali. *International Journal of Remote Sensing and Earth Sciences* 6 (1): 39-45.
- Hendrawan, I. G., K. Asai. 2014. Numerical study on tidal currents and seawater exchange in the Benoa Bay, Bali, Indonesia. *Acta Oceanologica Sinica*, 33 (3): 90-100.
- Hendrawan, I. G., D. Uniluha., I. P. R. F. Maharta. 2016. Characteristics of Total Suspended solids (Total Suspended Solid) and turbidity (Turbidity) operates vertically in Gulf waters Benoa, Bali. *Journal of Marine and Aquatic Science* 2: 29-33.
- Jose, F., D. Kobashi, G.W. Stone. 2007. Spectral Wave Transformation Over an Elongated Sand Shoal off South-Central Louisiana, USA. *J. Coast. Res.* S1 50 (Proceeding of the 9th International Coastal Symposium). 757-761. Gold Coast. Australia.
- Jun-zheng, Z. H. U., Y. U. Pu-bing. 2009. Numerical method for the storm tide overflow model in Hangzhou bay and Qiantangjiang estuary. *Journal Advances in Water Science* 2: 018.
- Kartadikaria, A. R., Y. Miyazawa, S. M. Varlamov., K. Nadaoka. 2011.

- Ocean circulation for the Indonesian seas driven by tides and atmospheric forcing: Comparison to observational data. *Journal of Geophysical Research: Oceans*, 116 (C9): 1-21.
- Lazure, P., V. Garnier, F. Dumas, C. Herry., M. Chifflet. 2009. Development of a hydrodynamic model of the Bay of Biscay. Validation of hydrology. *Continental Shelf Research* 29 (8): 985-997.
- Meylan, M. H., Bennetts, L. G., Kohout, A. L. 2014. In situ measurements and analysis of ocean waves in the Antarctic marginal ice zone. *Geophysical Research Letters* 41 (14): 5046-5051.
- Ningsih, N. S., Al Azhar, M. 2013. Modelling of hydrodynamic circulation in Benoa Bay, Bali. *Journal of Marine Science and Technology* 18 (2): 203-212.
- Ondara, K., Wisna, U. J. 2016. Numerical Simulation of Spectral Waves and Rob Disaster Using Flexible Mesh and Data Elevation Model in Waters of Sayung District, Demak. *Indonesian Journal of Marine Science and Technology* 9 (2):164-174.
- Qi, W. G., Gao, F. P. 2014. Physical modeling of local scour development around a large-diameter monopile in combined waves and current. *Coastal Engineering* 83: 72-81.
- Rachman, H. A., I. G. Hendrawan., I. D. N. N. Putra. 2016. Study of Sediment Transport in Benoa Bay Using Numerical Model. *Indonesian Journal of Marine Science and Technology* 9 (2): 144-154.
- Ricchiuto, M., Filippini, A. G. 2014. Upwind residual discretization of enhanced Boussinesq equations for wave propagation over complex bathymetries. *Journal of Computational Physics* 271: 306-341.
- Sato, S., Liu, H. 2013. A sheetflow sediment transport model for skewed-asymmetric waves combined with strong opposite currents. *Coastal Engineering* 71: 87-101.
- Triatmodjo, B. 2012. Coastal Building Planning. Beta Offset. Yogyakarta. Indonesia.
- Warner, J. C., B. Armstrong, R. He., J.B. Zambon. 2010. Development of a coupled ocean-atmosphere-wave-sediment transport (COAWST) modeling system. *Ocean Modelling* 35 (3): 230-244.
- Wisha, U. J., Husrin, S., Prihantono, J. 2015. Hidrodinamika Perairan Teluk Banten Pada Musim Peralihan (Agustus-September). *Ilmu Kelautan: Indonesian Journal of Marine Sciences* 20 (2): 101-112.
- Wisha, U. J., M. Yusuf., L. Maslukah. 2016. Abundance of Phytoplankton and TSS Value as an Indicator for Porong River Estuary Water Conditions. *Indonesian Journal of Marine Science and Technology* 9 (2): 122-129.
- Wisha, U. J., T. Al Tanto, W. S. Pranowo., S. Husrin. 2018. Current Movement in Benoa Bay Water, Bali, Indonesia: Pattern of Tidal Current Changes Simulated for the Condition before, during, and after Reclamation. *Regional Studies in Marine Science* 18: 177-187.
- Zijlema, M., G. P. Van Vledder., L. H. Holthuijsen. 2012. Bottom friction and wind drag for wave models. *Coastal Engineering* 65: 19-26.